ENHANCEMENT OF CURRENT PEAK MULTIPLICITY RELATED TO CUPROUS OXIDE ELECTROREDUCTION AND TRANSIENT COPPER ACTIVATION IN ALKALINE SOLUTION

M.E. MARTINS and A.J. ARVÍA

Instituto de Investigaciones Fisicoquímicas Teóricas y Aplicadas, INIFTA, Casilla de Correo 16, Sucursal 4, 1900 La Plata (Argentina)

ABSTRACT

Anodic films formed on Cu electrodes immersed in 0.1 M NaOH in the Cu/Cu(I) potential range were subjected to combined triangular potential sweeps and then immediately electroreduced to confirm the multiplicity of the species anodically formed and to investigate the roughening and sintering processes at the metal surface. These two processes are tentatively related to the increase in the cathodic current in the hydrogen evolution potential range, a fact which is apparently due to the electrode surface morphology attained after the potential perturbation programme was applied to the electrode, as deduced from SEM patterns.

INTRODUCTION

The potentiodynamic E/I profile of Cu in alkaline solutions obtained between the potential region where hydrogen evolution takes place and the potential region related to electroformation of Cu_2O changes appreciably with the characteristics of the potential perturbation [1–5]. Thus, when the Cu_2O layer is electroformed by applying a potential sweep followed by a potential step to the electrode, various electroreduction current peaks related to the products formed during Cu_2O electroformation are observed in the first sweep in the negative potential direction instead of the single peak resulting when the electrode is perturbed with a triangular potential sweep. The peak multiplicity extends in the potential range where supposedly most of the Cu(I) species is electroreduced and hydrogen evolution takes place.

This paper describes the current peak multiplicity involved in the electroreduction of Cu(I) species when the potentiodynamic ageing perturbation technique [6] is applied to the electrode. This multiplicity apparently appears simultaneously with a considerable increase in current in the hydrogen evolution potential range. The latter effect has also been recently reported for gold in acid solutions and for silver in alkaline solutions, when these electrodes are subjected to the same type of potential perturbation [7,8]. In the present case, an attempt is also made to correlate the

electrochemical results with the morphology of the copper electrode surface as determined by SEM.

EXPERIMENTAL

A conventional three-compartment electrolysis Pyrex cell was used. Cu working electrodes were prepared from spectroscopic quality Cu wires (0.4 mm diameter). Electrode pretreatment consisted of first polishing with 400 mesh high purity alumina powder, then thorough rinsing with distilled water, and finally 15 s etching in 50% HNO_3 solution. This pretreatment gave reproducible results [2]. A large platinum sheet counter-electrode and a $Hg/HgO/0.1$ M NaOH reference electrode were used. All potentials are given against the normal hydrogen electrode. The electrolyte (0.1 M NaOH) was prepared from a.r. NaOH and triply distilled water. The solution was deaerated by bubbling purified nitrogen through the system before each run. Experiments were carried out at 30°C.

To attain the stabilized E/I profile, the electrode was initially perturbed with cyclic triangular potential sweeps (RTPS) at 0.2 V/s between $E_c = -1.29$ V and $E_a = -0.08$ V. Afterwards, the potentiodynamic ageing perturbation programme [6,7] was applied to the electrode for a certain time, τ (number of cycles, n); the corresponding intermediate triangular potential sweeps (IRTPS) covered from E_c' (-0.49 V $< E_c' < -0.36$ V) to E_a (-0.19 V $< E_a < -0.08$ V). The last IRTPS was followed by two complete TPS between E_c and E_a. The corresponding $E/$time diagram is depicted in each figure. The circuitry was the same as that used in previous work [4].

SEM photographs of the electrode surface were obtained from: (i) the recently polished electrode without electrochemical treatment; (ii) the electrode when the stabilized RTPS E/I profile had been attained; (iii) the electrode after it was subjected to a pre-set number (n) of IRTPS; and (iv) the electrode which immediately after perturbation indicated by (iii) was further subjected to RTPS to recover the stabilized E/I profile.

RESULTS

The stabilized RTPS E/I profile run at 0.2 V/s covering from $E_c = -1.29$ V to $E_a = -0.08$ V exhibited a broad anodic current peak (API) located at ca. -0.14 V and another broad cathodic current peak (CPI) at ca. -0.46 V (Fig. 1a) [1–4]. This E/I profile serves as a comparison to those resulting under the complex potential perturbation conditions.

After the electrodes had been subjected to potentiodynamic ageing perturbation between E_c' and E_a, the complete electroreduction E/I profile from E_a to E_c resulting immediately afterwards (Fig. 1b, curve 1) showed a net increase in charge, a new cathodic current peak (CPT) whose peak potential was much more negative than that of CPI, and a considerable increase in current in the hydrogen evolution potential range. However, when the potential limits of the RTPS were reset at
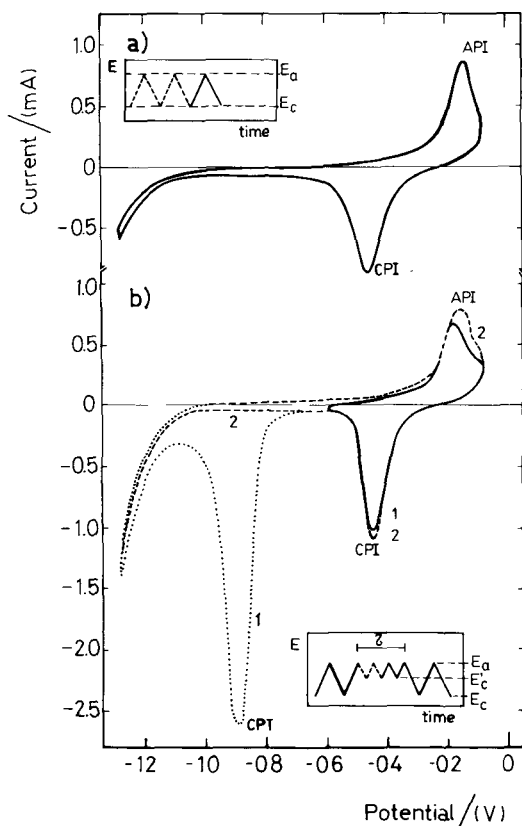
Fig. 1. Potentiodynamic E/I profiles. 0.2 V/s, 0.1 M NaOH, 0.52 cm^2 apparent electrode area, 25°C. (a) Stabilized E/I profile; (b) with IRTPS E/I profile. ($\cdots\cdots$) first TPS and (— — —) second TPS both run after the IRTPS. $E_a = -0.08$ V, $E_c = -1.29$ V, $E_c' = -0.59$ V, $\tau = 12$ min.

$E_a = -0.08$ V and $E_c = -1.29$ V, CPT disappeared and the initial stabilized E/I profile was gradually reached (Fig. 1b, curve 2), although the overall charge remained greater than that of the initial stabilized E/I profile, and the potential of API was shifted towards more positive potentials. The initial stabilized E/I profile was only obtained after a prolonged RTPS between E_c and E_a. The corresponding time depended on E_c', E_a and n.

For pre-set E_c' and E_a values, the heights of both API and CPI decreased as n increased (Fig. 2). Furthermore, there was progressive passivation of the electrode as n increased. The number of cycles required for complete passivation depended on E_c' and E_a. In this case, the potential of API remained constant and that of CPI moved towards more negative values.

On the other hand, when E_a was set at values more negative than -0.13 V, a reversible couple (couple I) in the -0.25 to -0.30 V potential range was observed and it became more clearly defined as n increased (Fig. 3). This redox couple, which is apparently the same as that described in previous investigations [2,5], has been
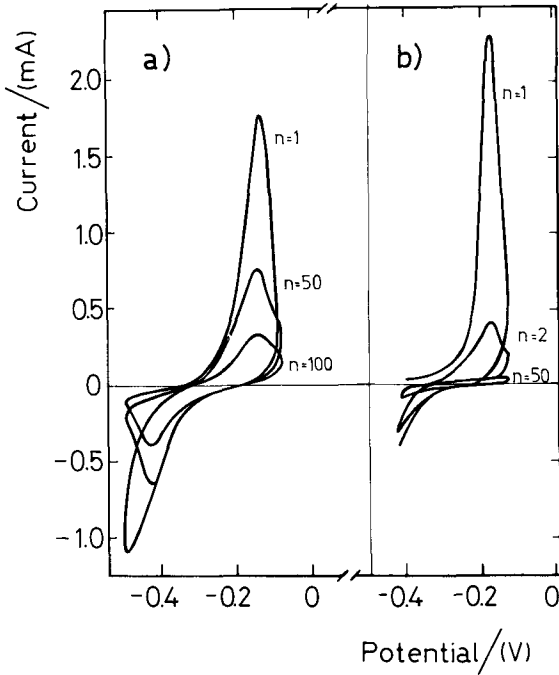
Fig. 2. IRTPS E/I profiles. 0.2 V/s, 0.1 M NaOH, 0.85 cm^2 apparent electrode area, 30°C. $E_a = -0.08$ V. (a) $E_c' = -0.50$ V; (b) $E_c' = -0.36$ V.
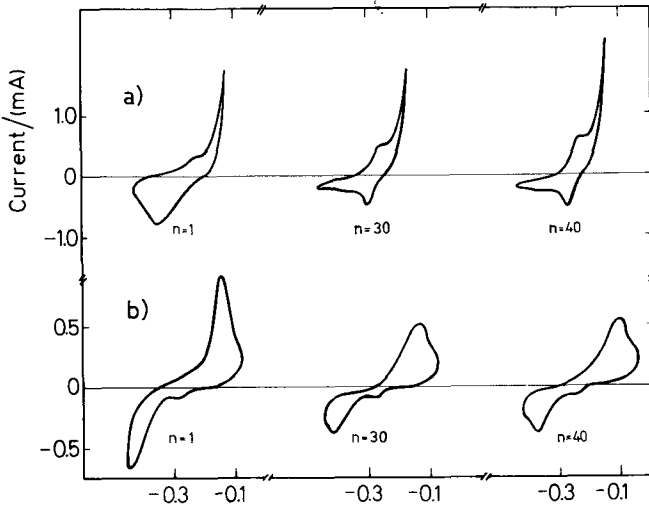

Fig. 3. IRTPS E/I profiles. 0.2 V/s, 0.1 M NaOH, 0.79 cm^2 apparent electrode area, 30°C. (a) $E_a = -0.16$ V, $E_c' = -0.46$ V; (b) $E_a = -0.08$ V, $E_c' = -0.46$ V.
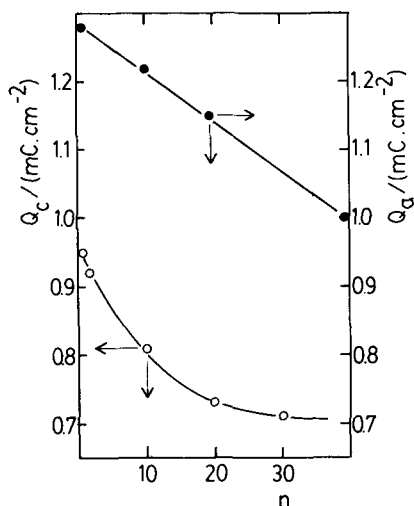
Fig. 4. Dependence of Q_c (○) and Q_a (●) on n. 0.1 M NaOH, 0.39 cm^2 apparent electrode area, 30°C.

confirmed throughout runs made with vitreous carbon/Cu(OH)$_2$ electrodes immersed in alkaline solutions [4].

The charge of IRTPS decreased during cycling but the anodic charge (Q_a) was always greater than the cathodic charge (Q_c) (Fig. 4). The complex nature of CPT can be visualized by an appropriate change in the potential perturbation parameters. For pre-set E_a, E_c and v values, the complete electroreduction profile run immediately after the IRTPS depended considerably on both E_c' and n, as clearly seen by comparing the profiles shown in Fig. 5. The plots of E_{CPT} vs. n and I_{CPT} vs. n (Fig. 6) indicate that the height of CPT increased and its peak potential gradually shifted towards more negative potentials as n increased.

On the other hand, at constant E_a and n, the symmetry, the charge and the peak potential of CPT changed in a complex way with E_c'. Thus, when E_c' was more negative than -0.50 V only one peak was observed, but as E_c' became more positive than -0.41 V the peak multiplicity in the electroreduction E/I profile was recorded. Otherwise, a further increase in E_c' beyond -0.36 V again produced an electroreduction profile with only a single peak at ca. -0.7 V (Fig. 5). The charge of CPT, estimated from the charge difference $\sum_0^n Q_a - \sum_0^n Q_c$ increased linearly with n ($0 < n < 40$) (Fig. 7). Likewise, for a constant n as E_c' became more positive, first a charge increase in CPT was noticed but the reverse occurred when E_c' extended beyond -0.36 V. The most remarkable splitting of the electroreduction E/I profile and charge difference were accomplished for $E_a = -0.16$ V, $E_c' = -0.41$ V and $n \simeq 40$. Otherwise, for $E_c' = -0.37$ V, CPT exhibited a shoulder at the negative potential side and for $E_c' = -0.46$ V, the latter turned into a new cathodic peak (Fig. 8). Therefore, CPT splits into various peaks whose peak potentials were at ca. -0.78 V (CPI') and -0.88 V (CPII) (Fig. 8). When E_c' exceeded -0.41 V, the height of CPII increased while that of CPI' decreased.
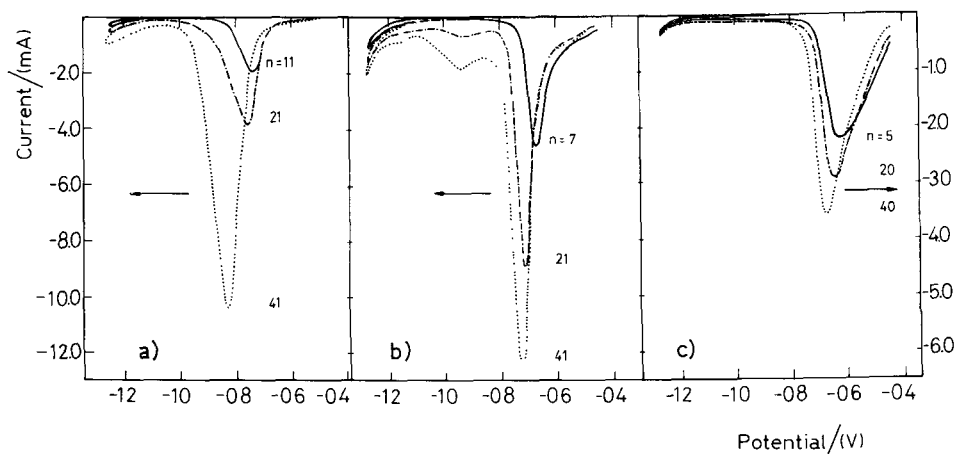
Fig. 5. Influence of τ on the electroreduction E/I profile. $E_a = -0.08$ V. 0.1 M NaOH. (a) $E_c' = -0.50$ V, 0.39 cm^2 apparent electrode area, (———) $n = 11$, ($-\cdot-\cdot$) $n = 21$, ($\cdots\cdots$) $n = 41$; (b) $E_c' = -0.41$ V, 0.86 cm^2 apparent electrode area, (———) $n = 7$, ($-\cdot-\cdot$) $n = 21$, ($\cdots\cdots$) $n = 41$; (c) $E_c' = -0.36$ V, 0.86 cm^2 apparent electrode area, (———) $n = 5$, ($-\cdot-\cdot$) $n = 20$, ($\cdots\cdots$) $n = 40$, 30°C.
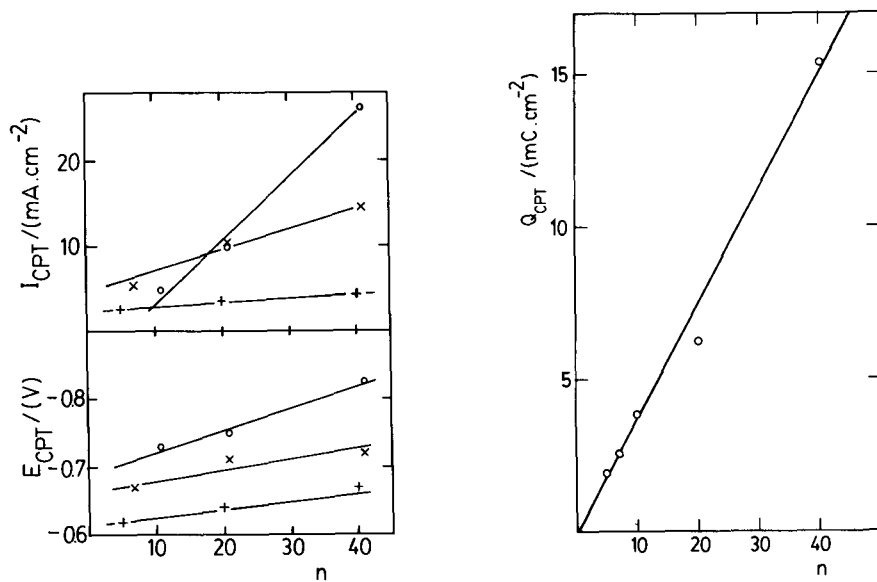

Fig. 6. Influence of n of E_{CPT} and I_{CPT}. 0.1 M NaOH. $E_a = -0.08$ V; $E_c' = -0.50$ V (○), 0.39 cm^2 apparent electrode area; $E_c' = -0.41$ V (×), 0.86 cm^2 apparent electrode area; and $E_c' = -0.36$ V (+), 0.86 cm^2 apparent electrode area, 30°C.

Fig. 7. Influence of n on the CPT. $E_c' = -0.66$ V; $E_a = -0.08$ V. 0.1 M NaOH, 0.39 cm^2 apparent electrode area, 30°C.
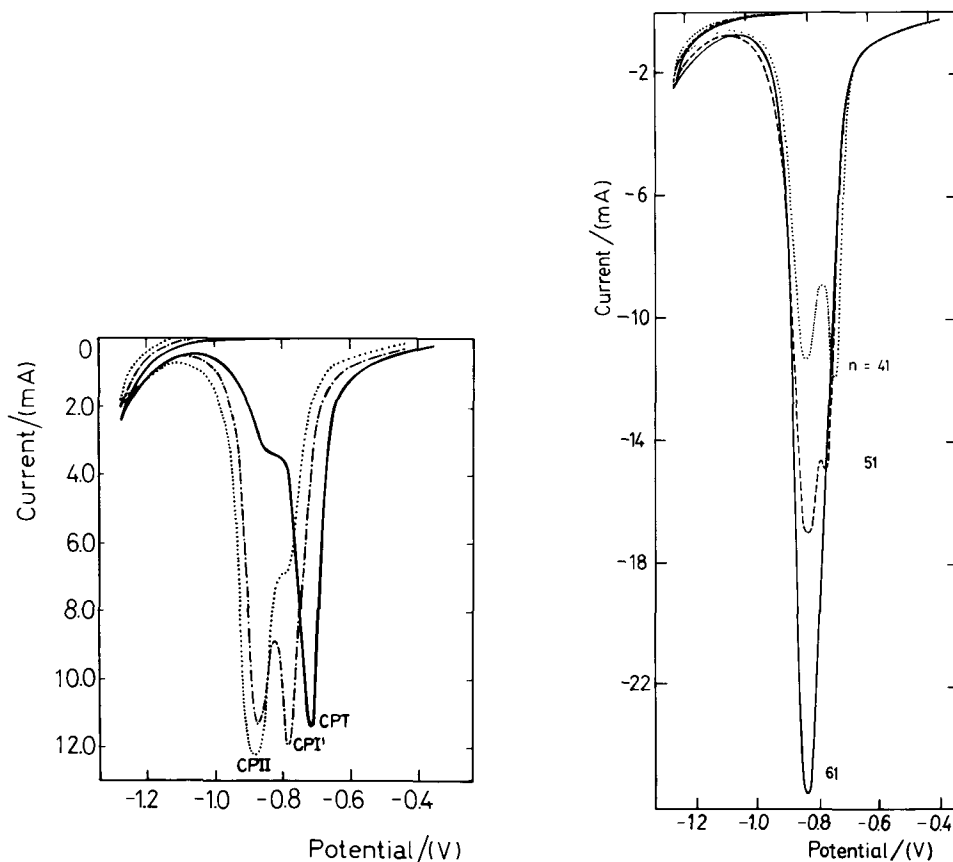
Fig. 8. Influence of E'_c on the electroreduction profiles. $n = 41$; $E_a = -0.16$ V. 0.1 M NaOH. 0.79 cm^2 apparent electrode area, 30°C. (————) $E'_c = -0.37$ V; (· · · · · ·) $E'_c = -0.46$ V; (· — · — ·) $E'_c = -0.62$ V.

Fig. 9. Influence of n on the electroreduction E/I profiles. $E_a = -0.16$ V; $E'_c = -0.62$ V. 0.1 M NaOH. 0.79 cm^2 apparent electrode area, 30°C. (· · · · · ·) $n = 41$, (— — —) $n = 51$, (————) $n = 61$.

When E'_c was in the -0.41 V $< E'_c < -0.50$ V range, after the IRTPS a progressive increase in the current in the hydrogen evolution potential range was also noticed. This effect was no longer observed when $E'_c > -0.36$ V.

Similar changes in the electroreduction profile were accomplished by increasing n, that is the duration of the IRTPS. Thus, the contribution of the shoulder in CPT increased with τ, resulting in a new current peak at -0.84 V. The height of the latter gradually increased with n, while that of CPI decreased and finally disappeared (Figs. 8 and 9). This splitting appeared only for -0.39 V $> E'_c > -0.44$ ($E_a = -0.16$ V).

The SEM pictures (Fig. 10) show an increase in the roughness of the electrode surface caused by the IRTPS. This effect is probably associated with the decrease in the average size of crystallites forming the anodic film.
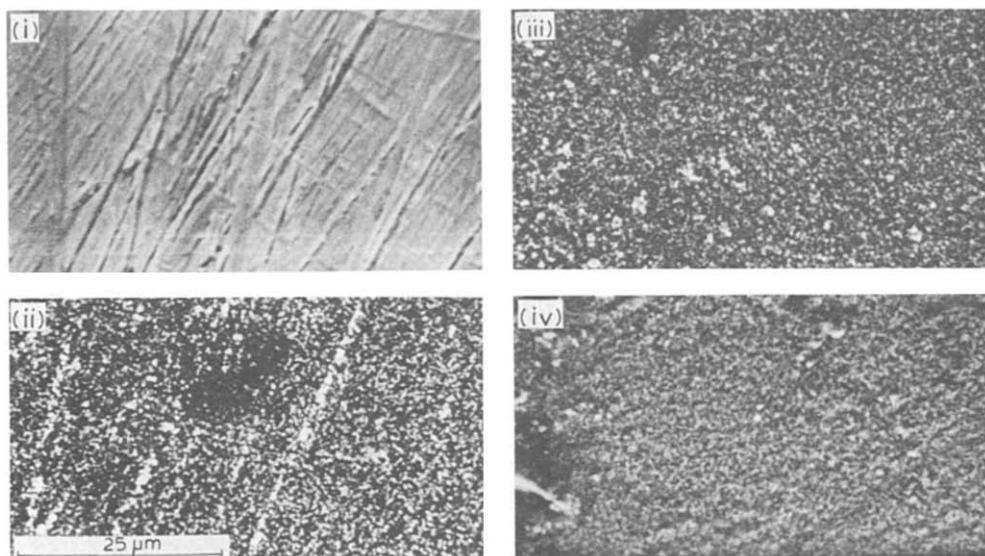
Fig. 10. SEM photographs obtained from (i) a recently polished electrode without electrochemical treatment; (ii) an electrode after the stabilized RTPS E/I profile had been attained; (iii) an electrode after $n = 1260$ IRTPS cycles (1 h 45 min) at $E_a = -0.2$ V, $E'_c = -0.7$ V, $v = 0.2$ V/s, $n = 1260$ cycles; (iv) an electrode which immediately after the perturbation indicated in (iii) was further subjected to RTPS to recover the stabilized RTPS E/I profile.

DISCUSSION

When copper electrodes are anodized in the potential range where Cu(I) species are formed, the potentiodynamic electroreduction response depends on the potential perturbation programme. Thus, it is possible to apply to the electrode: (i) a simple RTPS [1]; (ii) a positive potential step preceding the positive potential sweep [3]; (iii) a potential step included during the positive sweep to complete the formation of Cu_2O under constant potential conditions [3]; and (iv) a potentiodynamic ageing potential programme [6]. In all these cases, except (i), the electroreduction potentiodynamic E/I profile exhibits a multiplicity of peaks which depends on the proper characteristics of the perturbation programme.

The application of potentiodynamic ageing perturbation programmes to Cu electrodes in alkaline solutions in the potential range corresponding to electroformation of Cu(I) species produces a multiplicity of peaks in the electroreduction E/I profile when the sweep is extended from the Cu_2O electroformation potential range to that of hydrogen evolution. These changes in electroreduction profile are comparable to those already described under other potential perturbation conditions [2,3].

The strong dependence of the electrochemical response of Cu electrodes on the characteristics of the potential perturbation programme explains the difficulty of a

mechanistic interpretation of the kinetics of the electrode processes as well as the number of reaction models which were put forward to account for the data obtained in the Cu/Cu(I) potential range [3]. Previous studies concluded from the multiple peaks found in the electroreduction potentiodynamic E/I profile [2] that soluble Cu(I) and Cu(II) species are produced during electroformation of the complex Cu(OH)$_{ad}$ and Cu$_2$O layers.

Basically, data derived from the combined TPS used in this work can be analysed either in terms of the E/I profile variation during each successive IRTPS or in terms of the overall electroreduction E/I profile resulting immediately after the IRTPS perturbation was applied. The main difference between these analyses lies in the anodic charge taking part during the corresponding perturbation, which in the former is a film of the order of one monolayer thickness, while in the latter it corresponds to a relatively thin multilayer. In this case, the maximum in the multiplicity and the distribution of the cathodic charge among the various peaks are associated with relatively restricted ranges of n, E'_c and E_a values, namely when the charge of either Cu(OH)$_{ad}$ or Cu$_2$O involved in each IRTPS corresponds to the average thickness of a monolayer or a few monolayers. On the other hand, as the thickness of the anodic layer increases, as measured through the overall electroreduction charge, a gradual increase in the contribution of CPT is recorded. Then potential of CPT and the multiplicity distribution of the electroreduction profile depend on the amount of oxide electroformed during the IRTPS.

The roughness of the electrode increases to reach a maximum value, which depends on the IRTPS characteristics and on n. But the electrode roughness is apparently smeared out by RTPS covering the potential range between that of the Cu$_2$O electroformation and the potential range of the hydrogen evolution (Fig. 1). In this case, it appears that surface roughness and sintering are competitive processes occurring during the Cu(I) + e^- = Cu reaction. This conclusion correlates with the sequence of SEM photographs of the surface (Fig. 10), which show randomly distributed spheres on the surface, the sphere diameter being ca. 50 nm. The spheres change into a continuous rough surface when the IRTPS is followed by a RTPS, as already described. Processes such as Cu surface reconstruction and roughening, which are apparently emphasized through the application of IRTPS, should be related to re-accommodation of Cu and O atoms and to electroadsorption/electrodesorption of OH$^-$ ions during the potential cycling.

If one admits that the IRTPS increases the roughness of the electrode, the initial stages in the formation of the anodic layer can be explained provided that different active sites on the electrode surface, such as those in planes, at the borders of steps, in the bottom of holes, etc., participate in the reaction. This should imply an instantaneous non-equilibrium situation of different O-containing species as well as Cu itself, during both the electrooxidation and the electroreduction processes. During the electroreduction process the IRTPS promotes a large surface concentration of non-equilibrium (Cu*) species, which in the time scale of the potential perturbation are unable to attain thermal equilibrium conditions [9]. The Cu* species exhibits, in principle, a reactivity greater than that of the equilibrated Cu

species. This species can, in principle, be considered responsible for the apparent increase in the H_2 evolution current on the freshly formed Cu surface. This effect, however, can be related either to the increase in roughness or to the proper characteristics of the fresh Cu* surface formed from electroreduction of the O-containing Cu species.

On the other hand, the increase in cathodic current takes place simultaneously with the appearance of the reversible couple (couple I) preceding the main anodic current peak. This couple is related to the reaction [4]:

$$Cu^* + OH^- \rightleftarrows Cu^*(OH)_{ad} + e^- \tag{1}$$

where Cu* denotes a Cu atom under non-equilibrium conditions at the surface. In this case, the electrochemical response of the Cu surface after the IRTPS is similar to that observed for thin copper layer electrodes [4]. Moreover, reaction (1) may contribute to Cu* deactivation, as earlier suggested, through a reaction such as

$$Cu^*(OH)_{ad} \rightleftarrows Cu(OH)_{ad} \tag{2}$$

Furthermore, the deactivation of Cu* should also occur through re-accommodation in the lattice:

$$Cu^* \rightleftarrows Cu(lattice) \tag{3}$$

This reaction is to a great extent associated with the sintering effect [10–12]. The rate of reaction (3) should depend on the concentration of the Cu* species, although the specific rate constant regarded as similar to that deduced from the rate of thermal equilibration is apparently low.

The transient formation of Cu* explains the increase in current in the hydrogen evolution potential range which is beyond that expected from the roughness effect. This apparent activation of the hydrogen evolution reaction can be expressed by the following reaction:

$$Cu^* + H_2O + e^- \rightleftarrows Cu^*(OH)_{ad}^- + \tfrac{1}{2} H_2 \tag{4}$$

This type of activation for the hydrogen evolution reaction has already been observed for Au in acid electrolytes [7] and for Ag in alkaline solutions [8]. In principle, reaction (4) should be facilitated by the greater interaction between Cu* and H_2O within a potential range which probably lies close to the potential of zero charge of Cu in the electrolyte solution.

Finally, it is worthwhile mentioning that both the enhancement multiplicity of the electroreduction profile and the cathodic current in the hydrogen evolution potential range as seen in gold, silver and copper through the application of the combined triangular potential sweep perturbation appears, in principle, to be related to the formation of small spherical particles of fairly constant diameter packed together on the electrode. The sphere diameters are, in principle, in the order of those found for gold, silver and copper electrodes to produce an efficient enhancement of the corresponding Raman spectra [13]. This encourages a study to establish a quantitative correlation between the corresponding electrochemical and optical results.

REFERENCES

1 A.M. Castro Luna de Medina, S.L. Marchiano and A.J. Arvia, J. Appl. Electrochem., 8 (1978) 121.
2 S.L. Marchiano, C.I. Elsner and A.J. Arvia, J. Appl. Electrochem., 10 (1980) 365.
3 M.R. Gennero de Chialvo, S.L. Marchiano and A.J. Arvia, J. Appl. Electrochem., in press.
4 M.R. Gennero de Chialvo, S.L. Marchiano and A.J. Arvia, in preparation.
5 J.M.M. Droog, C.A. Alderstein, P.T. Alderstein and G.A. Bootsma, J. Electroanal. Chem., 111 (1970) 61.
6 M.E. Folquer, J.O. Zerbino, N.R. de Tacconi and A.J. Arvia, J. Electrochem. Soc., 126 (1979) 592.
7 R. Córdova O., M.E. Martins and A.J. Arvia, J. Electrochem. Soc., 127 (1980) 2628.
8 G.I. Lacconi and A.S. Gioda, Resúmenes extendidos del XVI Congreso Argentino de Química, Córdoba, 1982.
9 J.O'M. Bockris and E. Buck, Structure and Properties of Metal Surfaces, Maruzen, Tokyo, 1973.
10 P. Stonehart and P.A. Zucks, Electrochim. Acta, 17 (1972) 2333.
11 A.C.C. Tseung and S.C. Dhara, Electrochim. Acta, 20 (1975) 681.
12 A.E. Bolzán, M.E. Martins and A.J. Arvia, J. Electroanal. Chem., 157 (1983) 339.
13 C.C. Busby and J.A. Creighton, J. Electroanal. Chem., 140 (1982) 379.